

AN INNOVATIVE METHODOLOGY FOR ERROR ANALYSIS OF THERMO-FLUID SYSTEMS

David Dodoo-Amoo, Julio Mendez, Mookesh Dhanasar, Frederick Ferguson
Mechanical Engineering Department, North Carolina A&T State University
Greensboro 27411, USA

ABSTRACT

The physics that govern fluid flows are described by the conservation laws along with the appropriate initial and boundary conditions. Further, in fluid dynamics, the conservation laws are represented by a set of partial differential equations which do not readily lend themselves to analytical solutions. Nonetheless, the advent of computers allowed for the creation of Computational Fluid Dynamics (CFD), which is a field of study that is mainly focused on the numerical solution of these conservation laws. Today, these numerical solutions fall into one of the two major classes of numerical techniques: Finite Volume Method (FVM) and Finite Difference Method (FDM). Recently, a hybrid numerical technique, called the Integro-Differential Scheme (IDS), was developed and applied to a few problems without being fully tested. The IDS technique is worthy of a full technical evaluation as its preliminary results are impressive. As with any numerical technique, the IDS error capability must be rigidly analyzed, if the conservation principles, as well as, the physics capturing capability are to be credible. In lieu of analytical methods, this research seeks to study and quantify the IDS error behavior through an innovative numerical approach. Herein, selective 1D fluid dynamic problems are solved analytically and numerically with the use of the IDS technique. Further, orders of magnitude error analysis are conducted in both cases, and the results compared. In this research project, specialized numerical spline routines were developed that allows the IDS numerical solutions to be used as 'quasi-exact' solutions. This process facilitated the appropriate comparison of the two classes of solutions: analytical and 'quasi-exact' solutions. In this paper, the aforementioned error analysis procedure is described. In addition, to illustrate its effectiveness, a series of Quasi-1D convergent-divergent nozzle problems are analyzed, and the results reported herein. The numerical solution is compared to known values at specific locations in the nozzle to validate its use as 'quasi-exact'. The results show that the maximum error was 6.78% thus validating the use of the numerical solution as 'quasi-exact'.

INTRODUCTION

With the advent of the modern computers came numerous advances in physical problems involving fluid flow. The non-existence of analytical solutions to the differential equations governing fluid flow ceased to be a limitation to our ability to understand physics. Numerical schemes such as Finite difference methods(FDM), Finite volume methods(FVM) and Integro-Differential Scheme (IDS)[1] have been developed to solve the Navier Stokes Equations. However, these schemes inherently have the ability to introduce errors. The conventional way of measuring the accuracy of the solutions is to compare the numerical solution to an analytical exact solution or in some cases to experimental results. Analytical exact solutions however are not readily

available for numerous problems and boundary conditions so experimental results suffice though they may be expensive to conduct. The purpose of this paper is to describe the implementation of a new methodology to obtain a “Standard Solution” from our numerical results that can be considered the numerical exact solution. The numerical exact solution then takes the place of the analytical solution for error analysis. Outlined in Section 1 are the set of conservation equations that govern quasi 1-D fluid flow. Section 2 talks about choosing an appropriate numerical code that can solve sets of differential equations with no exact solution. Followed by section 3 which describes a standardized way of creating a Numerical Exact solution. Section 4 follows the principle of demonstrating that the numerical standard solution is good enough to replace the Exact Analytical Solution.

SECTION 1 GOVERNING DIFFERENTIAL EQUATIONS- QUASI 1D NAVIER STOKES EQUATIONS

The set of Navier-Stokes equations govern the physics of all fluid flows. To obtain a unique solution to a problem however, initial and boundary conditions must be specified. For the purpose of this paper, we use the quasi 1D form of the Navier-Stokes equations as applied to converging-diverging nozzles. This is given by

Conservation of Mass :

$$\frac{\partial(\rho A)}{\partial t} + \frac{\partial(\rho u A)}{\partial x} = 0 \quad (1)$$

Conservation of Momentum :

$$\frac{\partial(\rho u A)}{\partial t} + \frac{\partial[(\rho u^2 + p)A]}{\partial x} - p \frac{dA}{dx} = 0 \quad (2)$$

Conservation of Energy :

$$\frac{\partial(\rho e_T A)}{\partial t} + \frac{\partial[(\rho e_T + p)u A]}{\partial x} = 0 \quad (3)$$

In order to reduce equations (1-3) to non-dimensional form, we introduce the following definitions.

$$\left\{ \begin{array}{l} \bar{T} = \frac{T}{T_o} \quad \bar{\rho} = \frac{\rho}{\rho_o} \quad \bar{P} = \frac{P}{P_o} \quad \bar{x} = \frac{x}{L} \\ \bar{u} = \frac{u}{a_o} \quad \bar{t} = \frac{t}{L/a_o} \quad \bar{e} = \frac{e}{e_o} \quad \bar{A} = \frac{A}{A^*} \end{array} \right. \quad (4)$$

Also the total speed of sound (a_o) and internal energy(e_o) at total conditions is defined as

$$a_o = \sqrt{\gamma RT_o} \rightarrow a_o^2 = \gamma RT_o \rightarrow RT_o = \frac{a_o^2}{\gamma} \quad (5)$$

$$e_o = c_v T_o = \frac{RT_o}{(\gamma - 1)} \quad (6)$$

The conservation equations become

Conservation of Mass :

$$\frac{\partial(\bar{\rho}\bar{A})}{\partial\bar{t}} + \frac{\partial(\bar{\rho}\bar{u}\bar{A})}{\partial\bar{x}} = 0 \quad (7)$$

Conservation of Momentum :

$$\frac{\partial(\bar{\rho}\bar{u}\bar{A})}{\partial\bar{t}} + \frac{\partial}{\partial\bar{x}} \left[\bar{\rho}\bar{A} \left(\bar{u}^2 + \frac{\bar{T}}{\gamma} \right) \right] - \frac{\bar{\rho}\bar{T}}{\gamma} \frac{d\bar{A}}{d\bar{x}} = 0 \quad (8)$$

Conservation of Energy :

$$\frac{\partial}{\partial\bar{t}} (\bar{\rho}\bar{e}_T\bar{A}) + \frac{\partial}{\partial\bar{x}} [\bar{\rho}\bar{u}\bar{A}(\bar{e}_T + \bar{T})] = 0 \quad (9)$$

Where $\bar{e}_T \stackrel{\text{def}}{=} \frac{\bar{e}}{(\gamma-1)} + \frac{\gamma}{2} \bar{u}^2$

In vector form, the non-dimensional form of the unsteady Quasi 1-D Navier Stokes Equations (7-9) can be written in the form given by equation (10)

$$\frac{\partial U}{\partial t} + \frac{\partial F}{\partial x} - G = 0 \quad (10)$$

Where the vectors, U, F and G are defined as

$$U = \begin{bmatrix} \rho A \\ \rho u A \\ \rho e_T A \end{bmatrix}, \quad F = \begin{bmatrix} \rho u A \\ \rho A \left(u^2 + \frac{T}{\gamma} \right) \\ \rho u A (e_T + T) \end{bmatrix} \quad \text{and} \quad G = \begin{bmatrix} 0 \\ \frac{\rho T}{\gamma} \frac{dA}{dx} \\ 0 \end{bmatrix}$$

SECTION 2 CHOOSING AN APPROPRIATE NUMERICAL SCHEME – INTEGRAL-DIFFERENTIAL SCHEME

The IDS was chosen as the appropriate numerical scheme to demonstrate this new methodology because of its success in overcoming limitations of well-established schemes and obtaining accurate solutions that most conventional schemes are not able to [1]. The IDS is a hybrid scheme that combines the advantages of both the finite difference methods and the finite volume methods [2], that is, it focuses on the evolution of fluxes hence maintaining the conservative nature of the governing equations, and the equations are easily discretized based on finite difference methods. For the 2-D version of it, the control volume is made up of 4 cells as shown in **Error! Reference source not found.**. The time derivatives at each cell center is evaluated using the mean value theorem. And then the time derivative for the control volume is evaluated at the center of the volume by an arithmetic average of the 4 neighboring cells. This averaging procedure is done consistently throughout the scheme.

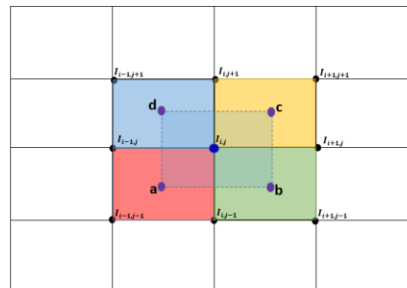


Figure 1. 2-Dimensional IDS control volume.

For this paper however, the quasi 1-D form of the IDS scheme is used.

SECTION 3 STANDARD SOLUTION (NUMERICALLY EXACT SOLUTION)

To obtain the standard solution, the quasi 1-D IDS was applied to 5 pairs of nozzle flow problems of varying nozzle geometries. For each pair, the initial condition was kept constant but the boundary conditions were altered so produce either an isentropic solution or a shock solution in the nozzle. This is to enable the testing of the scheme for both smooth and discontinuous solutions. Discontinuities are known to introduce errors into solutions which tend to grow with the evolution of the solution towards steady state.

3.1 Choosing Different Nozzle Geometries and Problems

1. Anderson nozzle [3]

Figure 2 and Figure 3 show the Anderson nozzle subject to Isentropic and Shock conditions respectively.

$$A(x) = 1.0 + 2.2(x - 1.5)^2$$

Problem ID1: Anderson Nozzle Isentropic Flow

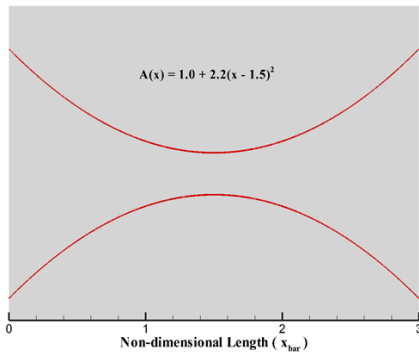


Figure 2: Anderson Nozzle Isentropic Flow

Problem ID2: Anderson Nozzle Shock Flow

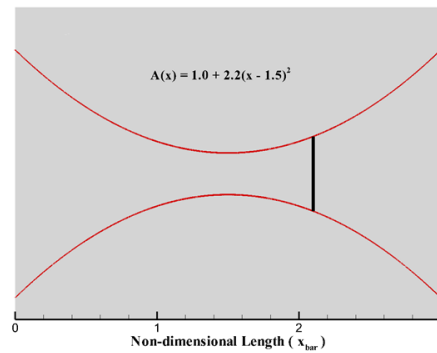


Figure 3: Anderson Nozzle for Shock flow

Initial Condition

Isentropic

$$\begin{bmatrix} \rho \\ u \\ T \end{bmatrix}_{x_{bar}}^{t=0} = \begin{bmatrix} 1.0 \\ 0.59/\rho A \\ 1.0 \end{bmatrix} \quad 0 \leq x_{bar} < 0.5,$$

$$\begin{bmatrix} \rho \\ u \\ T \end{bmatrix}_{x_{bar}}^{t=0} = \begin{bmatrix} 1.0 - 0.366(x_{bar} - 0.5) \\ 0.59/\rho A \\ 1.0 - 0.167(x_{bar} - 0.5) \end{bmatrix} \quad 0.5 \leq x_{bar} < 1.5$$

Shock

$$\begin{bmatrix} \rho \\ u \\ T \end{bmatrix}_{x_{bar}}^{t=0} = \begin{bmatrix} 1.0 \\ 0.59/\rho A \\ 1.0 \end{bmatrix} \quad 0 \leq x_{bar} < 0.5,$$

$$\begin{bmatrix} \rho \\ u \\ T \end{bmatrix}_{x_{bar}}^{t=0} = \begin{bmatrix} 1.0 - 0.366(x_{bar} - 0.5) \\ 0.59/\rho A \\ 1.0 - 0.167(x_{bar} - 0.5) \end{bmatrix} \quad 0.5 \leq x_{bar} < 1.5$$

$$\begin{bmatrix} \rho \\ u \\ T \end{bmatrix}_{x_{bar}}^{t=0} = \begin{bmatrix} 0.634 - 0.3879(x_{bar} - 1.5) \\ 0.59/\rho A \\ 0.833 - 0.3507(x_{bar} - 1.5) \end{bmatrix} \quad x_{bar} \geq 1.5$$

Inflow Conditions

Outflow Conditions

$$\begin{bmatrix} \rho \\ u \\ T \end{bmatrix}_{x_{bar}}^{t=0} = \begin{bmatrix} 0.634 - 0.3879(x_{bar} - 1.5) \\ 0.59/\rho A \\ 0.833 - 0.3507(x_{bar} - 1.5) \end{bmatrix} \quad x_{bar} \geq 1.5$$

Inflow Conditions

Outflow Conditions

$$\begin{bmatrix} \rho \\ u \\ T \end{bmatrix}_{i=1}^t = \begin{bmatrix} 1.0 \\ 2.0u_2 - u_3 \\ 1.0 \end{bmatrix} \quad \begin{bmatrix} \rho \\ u \\ T \end{bmatrix}_{i_{max}}^n = \begin{bmatrix} 2.0\rho_{(i_{max}-1)} - \rho_{(i_{max}-2)} \\ 2.0u_{(i_{max}-1)} - u_{(i_{max}-2)} \\ 2.0T_{(i_{max}-1)} - T_{(i_{max}-2)} \end{bmatrix}$$

$$\begin{bmatrix} \rho \\ u \\ T \end{bmatrix}_{i=1}^t = \begin{bmatrix} 1.0 \\ 2.0u_2 - u_3 \\ 1.0 \end{bmatrix} \quad \begin{bmatrix} \rho \\ u \\ T \end{bmatrix}_{i_{max}}^n = \begin{bmatrix} \rho_{i_{max}-1} \\ 0.1520 \\ T_{i_{max}-1} \end{bmatrix}$$

2. Absolute Nozzle

The Absolute nozzle is a modification of the Anderson nozzle to produce acute change in gradient at the throat of the nozzle. Figure 4 and Figure 5 show the Absolute nozzle subject to Isentropic and Shock conditions respectively.

$$A(x) = 1.0 + 5.3 \text{ abs}||x - 1.5||$$

Problem ID3: Absolute Nozzle Isentropic Flow

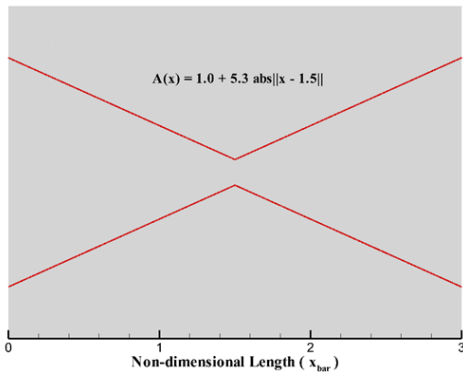


Figure 4: Absolute Nozzle Isentropic Flow

Problem ID4: Absolute Nozzle Shock Flow

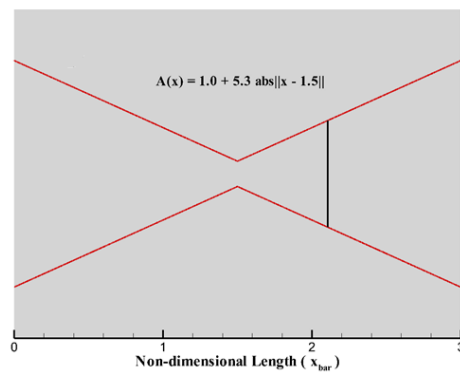


Figure 5: Absolute Nozzle for Shock flow

Initial Condition

Isentropic

$$\begin{bmatrix} \rho \\ u \\ T \end{bmatrix}_{x_{bar}}^{t=0} = \begin{bmatrix} 1.0 \\ 0.59/\rho A \\ 1.0 \end{bmatrix} \quad 0 \leq x_{bar} < 0.5,$$

$$\begin{bmatrix} \rho \\ u \\ T \end{bmatrix}_{x_{bar}}^{t=0} = \begin{bmatrix} 1.0 - 0.366(x_{bar} - 0.5) \\ 0.59/\rho A \\ 1.0 - 0.167(x_{bar} - 0.5) \end{bmatrix} \quad 0.5 \leq x_{bar} < 1.5$$

$$\begin{bmatrix} \rho \\ u \\ T \end{bmatrix}_{x_{bar}}^{t=0} = \begin{bmatrix} 0.634 - 0.3879(x_{bar} - 1.5) \\ 0.59/\rho A \\ 0.833 - 0.3507(x_{bar} - 1.5) \end{bmatrix} \quad x_{bar} \geq 1.5$$

Inflow Conditions

$$\begin{bmatrix} \rho \\ u \\ T \end{bmatrix}_{i=1}^t = \begin{bmatrix} 1.0 \\ 2.0u_2 - u_3 \\ 1.0 \end{bmatrix}$$

Outflow Conditions:

$$\begin{bmatrix} \rho \\ u \\ T \end{bmatrix}_{i_{max}}^n = \begin{bmatrix} 2.0\rho_{(i_{max}-1)} - \rho_{(i_{max}-2)} \\ 2.0u_{(i_{max}-1)} - u_{(i_{max}-2)} \\ 2.0T_{(i_{max}-1)} - T_{(i_{max}-2)} \end{bmatrix}$$

Shock

$$\begin{bmatrix} \rho \\ u \\ T \end{bmatrix}_{x_{bar}}^{t=0} = \begin{bmatrix} 1.0 \\ 0.59/\rho A \\ 1.0 \end{bmatrix} \quad 0 \leq x_{bar} < 0.5,$$

$$\begin{bmatrix} \rho \\ u \\ T \end{bmatrix}_{x_{bar}}^{t=0} = \begin{bmatrix} 1.0 - 0.366(x_{bar} - 0.5) \\ 0.59/\rho A \\ 1.0 - 0.167(x_{bar} - 0.5) \end{bmatrix} \quad 0.5 \leq x_{bar}$$

$$\begin{bmatrix} \rho \\ u \\ T \end{bmatrix}_{x_{bar}}^{t=0} = \begin{bmatrix} 0.634 - 0.3879(x_{bar} - 1.5) \\ 0.59/\rho A \\ 0.833 - 0.3507(x_{bar} - 1.5) \end{bmatrix} \quad x_{bar} \geq 1.5$$

Inflow Conditions

$$\begin{bmatrix} \rho \\ u \\ T \end{bmatrix}_{i=1}^t = \begin{bmatrix} 1.0 \\ 2.0u_2 - u_3 \\ 1.0 \end{bmatrix}$$

Outflow Conditions

$$\begin{bmatrix} \rho \\ u \\ T \end{bmatrix}_{i_{max}}^n = \begin{bmatrix} \rho_{i_{max}-1} \\ 0.1520 \\ T_{i_{max}-1} \end{bmatrix}$$

3. Feng Nozzle [3]

Figure 6 and Figure 7 show the Feng nozzle subject to Isentropic and Shock conditions respectively.

$$A(x) = 1.0 + 2.2(x - 1.50)^2 \quad \text{for } x \leq 1.5$$

$$A(x) = 1.0 + 0.2223(x - 1.50)^2 \quad \text{for } x > 1.5$$

Problem ID5: Feng Nozzle Isentropic Flow

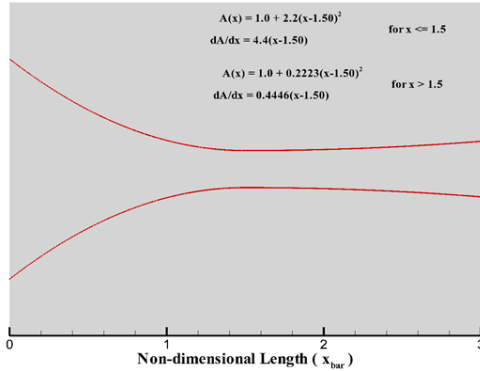


Figure 6: Feng Nozzle Isentropic Flow

Problem ID6: Feng Nozzle Shock Flow

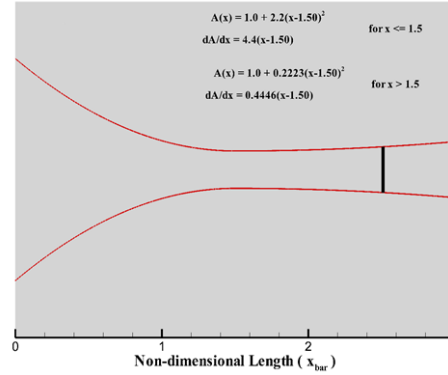


Figure 7: Feng Nozzle for Shock flow

Initial Condition

Isentropic

$$\begin{bmatrix} \rho \\ u \\ T \end{bmatrix}_{x_{bar}}^{t=0} = \begin{bmatrix} 1.0 \\ 0.59/\rho A \\ 1.0 \end{bmatrix}_{x_{bar}} \quad 0 \leq x_{bar} < 0.5,$$

$$\begin{bmatrix} \rho \\ u \\ T \end{bmatrix}_{x_{bar}}^{t=0} = \begin{bmatrix} 1.0 - 0.366(x_{bar} - 0.5) \\ 0.59/\rho A \\ 1.0 - 0.167(x_{bar} - 0.5) \end{bmatrix}_{x_{bar}} \quad 0.5 \leq x_{bar} < 1.5$$

$$\begin{bmatrix} \rho \\ u \\ T \end{bmatrix}_{x_{bar}}^{t=0} = \begin{bmatrix} 0.634 - 0.3879(x_{bar} - 1.5) \\ 0.59/\rho A \\ 0.833 - 0.3507(x_{bar} - 1.5) \end{bmatrix}_{x_{bar}} \quad x_{bar} \geq 1.5$$

Shock

$$\begin{bmatrix} \rho \\ u \\ T \end{bmatrix}_{x_{bar}}^{t=0} = \begin{bmatrix} 1.0 \\ 0.59/\rho A \\ 1.0 \end{bmatrix}_{x_{bar}} \quad 0 \leq x_{bar} < 0.5,$$

$$\begin{bmatrix} \rho \\ u \\ T \end{bmatrix}_{x_{bar}}^{t=0} = \begin{bmatrix} 1.0 - 0.366(x_{bar} - 0.5) \\ 0.59/\rho A \\ 1.0 - 0.167(x_{bar} - 0.5) \end{bmatrix}_{x_{bar}} \quad 0.5 \leq x_{bar} < 1.5$$

$$\begin{bmatrix} \rho \\ u \\ T \end{bmatrix}_{x_{bar}}^{t=0} = \begin{bmatrix} 0.634 - 0.3879(x_{bar} - 1.5) \\ 0.59/\rho A \\ 0.833 - 0.3507(x_{bar} - 1.5) \end{bmatrix}_{x_{bar}} \quad x_{bar} \geq 1.5$$

Inflow Conditions

$$\begin{bmatrix} \rho \\ u \\ T \end{bmatrix}_{i=1}^t = \begin{bmatrix} 1.0 \\ 2.0u_2 - u_3 \\ 1.0 \end{bmatrix}$$

Outflow Conditions:

$$\begin{bmatrix} \rho \\ u \\ T \end{bmatrix}_{i_{max}}^n = \begin{bmatrix} 2.0\rho_{(i_{max}-1)} - \rho_{(i_{max}-2)} \\ 2.0u_{(i_{max}-1)} - u_{(i_{max}-2)} \\ 2.0T_{(i_{max}-1)} - T_{(i_{max}-2)} \end{bmatrix}$$

Inflow Conditions

$$\begin{bmatrix} \rho \\ u \\ T \end{bmatrix}_{i=1}^t = \begin{bmatrix} 1.0 \\ 2.0u_2 - u_3 \\ 1.0 \end{bmatrix}$$

Outflow Conditions

$$\begin{bmatrix} \rho \\ u \\ T \end{bmatrix}_{i_{max}}^n = \begin{bmatrix} \rho_{(i_{max}-1)} \\ 0.48 \\ T_{(i_{max}-1)} \end{bmatrix}$$

4. Hoffmann Nozzle [4]

Figure 8 and Figure 9 show the Hoffmann nozzle subject to Isentropic and Shock conditions respectively.

$$A(x) = 1.5643 + 0.3883 \tanh(8x - 4)$$

Problem ID7: Hoffmann Nozzle Isentropic Flow

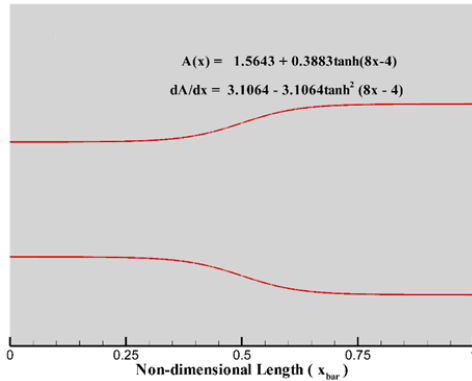


Figure 8: Hoffmann Nozzle for Isentropic Flow

Problem ID8: Hoffmann Nozzle Shock Flow

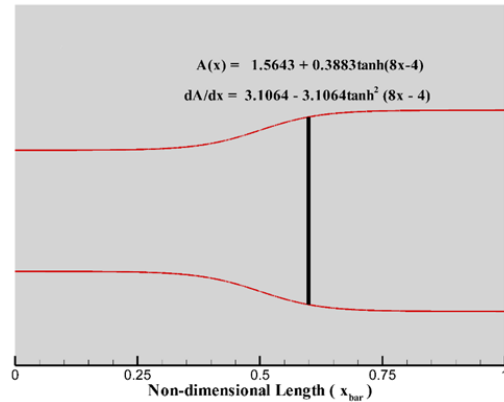


Figure 9: Hoffmann Nozzle for Shock Flow

Initial Condition

Isentropic

$$\begin{bmatrix} \rho \\ u \\ T \end{bmatrix}_i^{t=0} = \begin{bmatrix} 0.395 \\ 1.5 \times \sqrt{0.6897} \\ 0.6897 \end{bmatrix} \quad 0 \leq X_{bar} \leq 1$$

Shock

$$\begin{bmatrix} \rho \\ u \\ T \end{bmatrix}_i^{t=0} = \begin{bmatrix} 0.395 \\ 1.5 \times \sqrt{0.6897} \\ 0.6897 \end{bmatrix} \quad 0 \leq X_{bar} \leq 1$$

Isentropic

Shock

Inflow Conditions

$$\begin{bmatrix} \rho \\ u \\ T \end{bmatrix}_1 = \begin{bmatrix} 0.395 \\ 1.5 \times \sqrt{0.6897} \\ 0.6897 \end{bmatrix}$$

Outflow Conditions:

$$\begin{bmatrix} \rho \\ u \\ T \end{bmatrix}_{i_{max}} = 2 \begin{bmatrix} \rho \\ u \\ T \end{bmatrix}_{i_{max-1}} - \begin{bmatrix} \rho \\ u \\ T \end{bmatrix}_{i_{max-2}}$$

$$\begin{bmatrix} \rho^{(i_{max-1})} \\ 0.5081 \times \sqrt{T_{i_{max}}} \\ \rho^{(i_{max-1})} \end{bmatrix}$$

Inflow Conditions

$$\begin{bmatrix} \rho \\ u \\ T \end{bmatrix}_1 = \begin{bmatrix} 0.395 \\ 1.5 \times \sqrt{0.6897} \\ 0.6897 \end{bmatrix}$$

Outflow Conditions

$$\begin{bmatrix} \rho \\ u \\ T \end{bmatrix}_{i_{max}} =$$

5. Feng's 2nd Nozzle

Figure 10 and Figure 11 show the Feng's 2nd nozzle subject to Isentropic and Shock conditions respectively.

$$A(x) = 2.0 \quad \text{for } -1.0 \leq x < -0.5, \quad 0.5 \leq x \leq 1.0$$

$$A(x) = 1.0 + \sin^2(\pi x) \quad \text{for } -0.5 \leq x < 0.5$$

Problem ID9: Feng's 2nd Nozzle Isentropic Flow

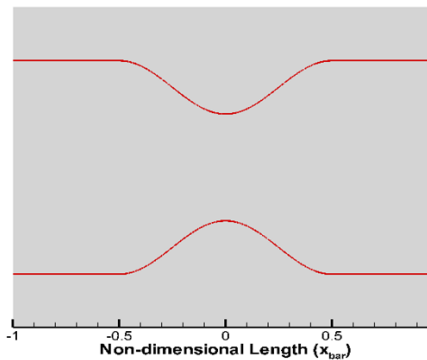


Figure 10: Feng's 2nd Nozzle Isentropic Flow

Problem ID10: Feng's 2nd Nozzle Shock Flow

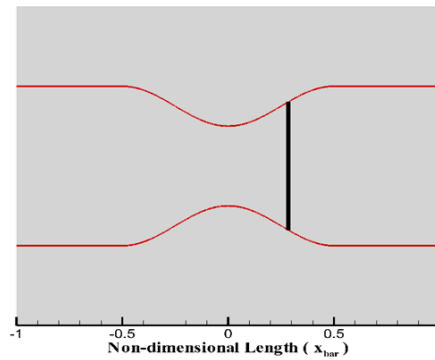


Figure 11: Feng's 2nd Nozzle for Shock flow

Initial Condition

Isentropic

Shock

$$\begin{bmatrix} \rho \\ u \\ T \end{bmatrix}_{x_{bar}}^{t=0} = \begin{bmatrix} 1.0 \\ 0.3 \\ 1.0 \end{bmatrix}_{x_{bar}} \quad x_{bar} < -0.5$$

$$\begin{bmatrix} \rho \\ u \\ T \end{bmatrix}_{x_{bar}}^{t=0} = \begin{bmatrix} 1.0 \\ 0.3 \\ 1.0 \end{bmatrix}_{x_{bar}} \quad x_{bar} < -0.5$$

Isentropic

$$\begin{bmatrix} \rho \\ u \\ T \end{bmatrix}_{x_{bar}}^{t=0} = \begin{bmatrix} 1.0 - 0.366(x_{bar} - 0.5) \\ 0.7 \\ 1.0 - 0.167(x_{bar} - 0.5) \end{bmatrix}_{x_{bar}} \quad -0.5 \leq x_{bar} < 0.5$$

Shock

$$\begin{bmatrix} \rho \\ u \\ T \end{bmatrix}_{x_{bar}}^{t=0} = \begin{bmatrix} 1.0 - 0.366(x_{bar} - 0.5) \\ 0.7 \\ 1.0 - 0.167(x_{bar} - 0.5) \end{bmatrix}_{x_{bar}} \quad -0.5 \leq x_{bar} < 0.5$$

$$\begin{bmatrix} \rho \\ u \\ T \end{bmatrix}_{x_{bar}}^{t=0} = \begin{bmatrix} 0.634 - 0.3879(x_{bar} - 1.5) \\ 1.5 \\ 0.833 - 0.3507(x_{bar} - 1.5) \end{bmatrix}_{x_{bar}} \quad 0.5 \leq x_{bar} \leq 1.0$$

$$\begin{bmatrix} \rho \\ u \\ T \end{bmatrix}_{x_{bar}}^{t=0} = \begin{bmatrix} 0.634 - 0.3879(x_{bar} - 1.5) \\ 1.5 \\ 0.833 - 0.3507(x_{bar} - 1.5) \end{bmatrix}_{x_{bar}} \quad 0.5 \leq x_{bar} \leq 1.0$$

Inflow Conditions

$$\begin{bmatrix} \rho \\ u \\ T \end{bmatrix}_{i=1}^t = \begin{bmatrix} 1.0 \\ 2.0u_2 - u_3 \\ 1.0 \end{bmatrix}$$

Outflow Conditions:

$$\begin{bmatrix} \rho \\ u \\ T \end{bmatrix}_{i_{max}}^n = \begin{bmatrix} 2.0\rho_{(i_{max}-1)} - \rho_{(i_{max}-2)} \\ 2.0u_{(i_{max}-1)} - u_{(i_{max}-2)} \\ 2.0T_{(i_{max}-1)} - T_{(i_{max}-2)} \end{bmatrix}$$

Inflow Conditions

$$\begin{bmatrix} \rho \\ u \\ T \end{bmatrix}_{i=1}^t = \begin{bmatrix} 1.0 \\ 2.0u_2 - u_3 \\ 1.0 \end{bmatrix}$$

Outflow Conditions

$$\begin{bmatrix} \rho \\ u \\ T \end{bmatrix}_{i_{max}}^n = \begin{bmatrix} \rho_{(i_{max}-1)} \\ 0.43 \\ T_{(i_{max}-1)} \end{bmatrix}$$

3.2 Distributed (Entire Nozzle)

Verification of the numerical solution is done by comparing qualitatively known physical phenomena that occur over the entire nozzle. For isentropic flow, total temperature and total pressure remain constant. However, for shock flow the total pressure decreases across the shock. For the various nozzle geometries subjected to isentropic and shock flow, Figures 12-16 show that the total temperatures and pressures behave as expected.

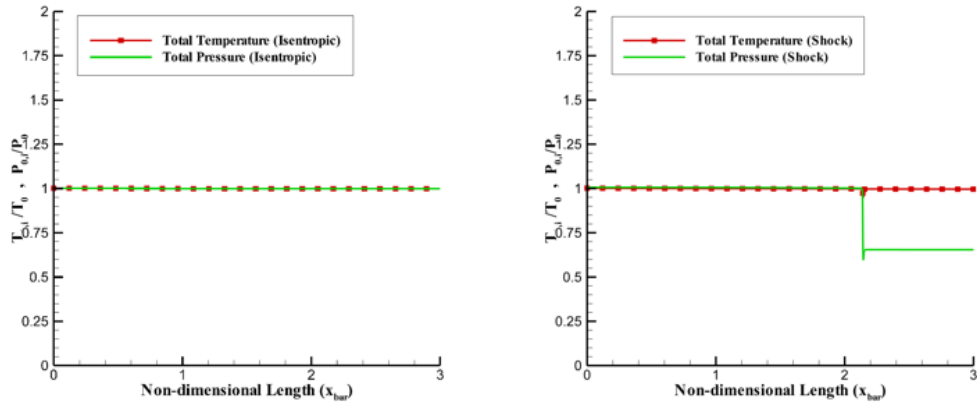


Figure 12. Total temperature and Total Pressure for Problem ID 1 (isentropic) and Problem ID 2 (Shock).

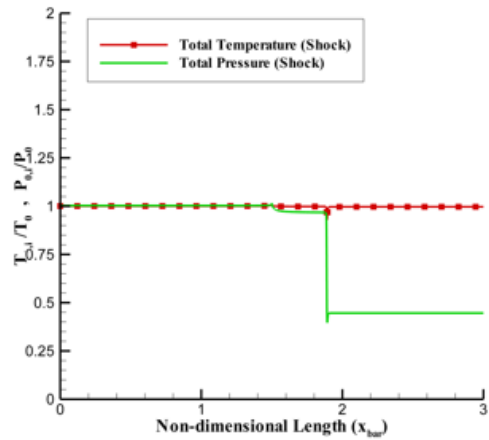
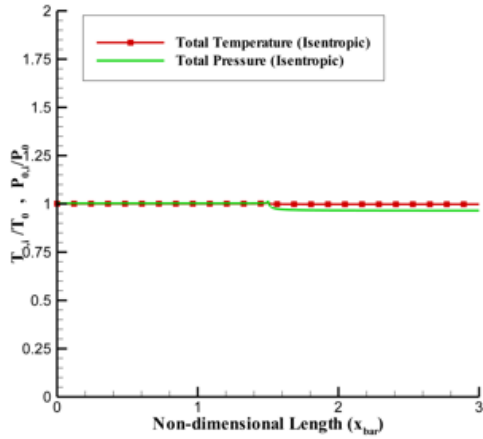


Figure 13. Total temperature and Total Pressure for Problem ID 3 (isentropic) and Problem ID 4 (Shock).

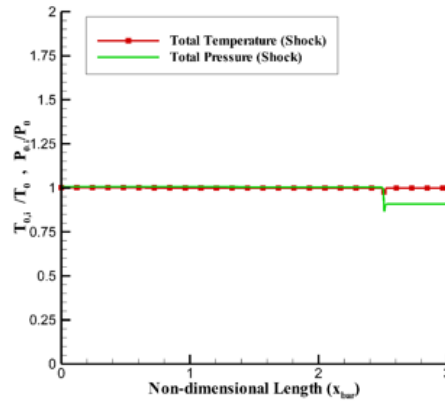
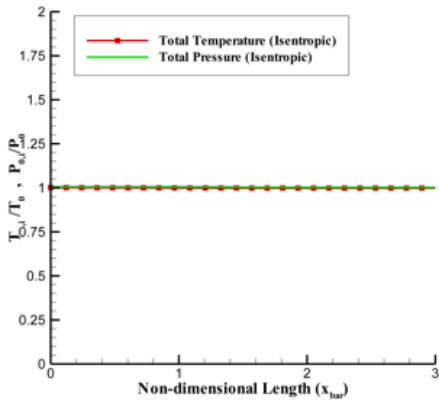


Figure 14. Total temperature and Total Pressure for Problem ID 5 (isentropic) and Problem ID 6 (Shock).

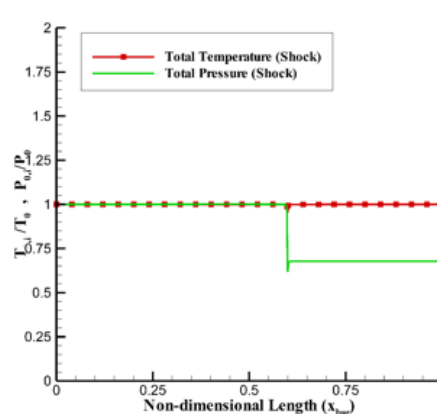
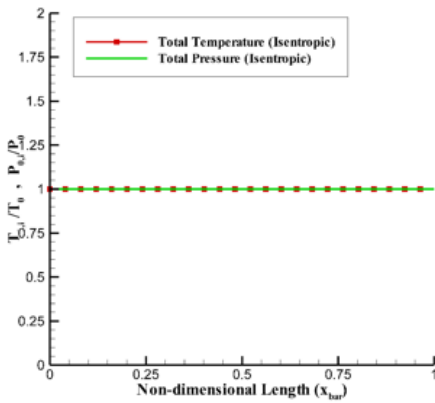


Figure 15. Total temperature and Total Pressure for Problem ID 7 (isentropic) and Problem ID 8 (Shock).

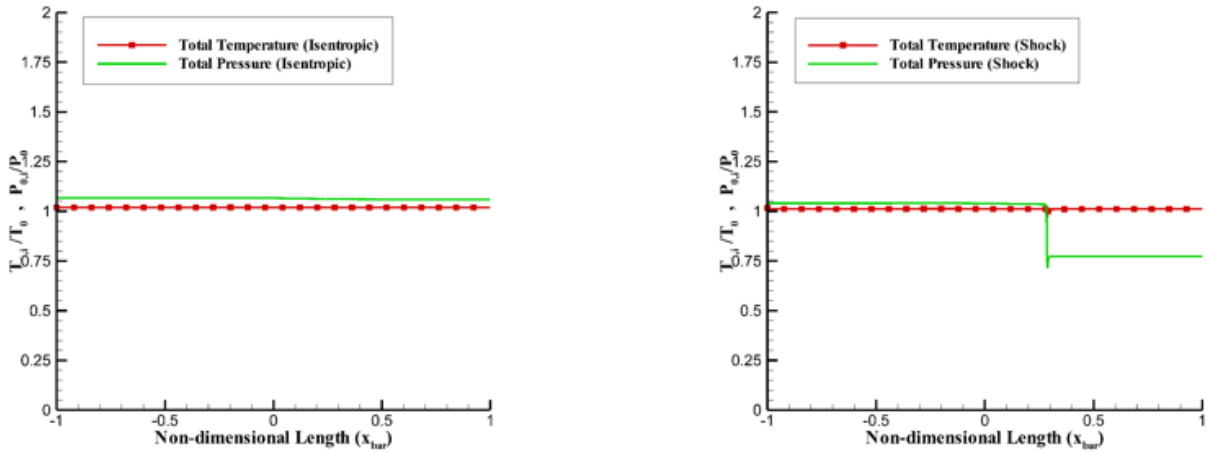


Figure 16. Total temperature and Total Pressure for Problem ID 9 (isentropic) and Problem ID 10 (Shock).

3.3 Pointwise Location

In order to validate the numerical solution, it is required that exact values are known at certain discrete points of the nozzle. One such location is the throat of the nozzle as shown in Figure 17. Let * denote any property at the throat of the nozzle as is normally used in scientific literature. The non-dimensional quantities T^*/T_0 , P^*/P_0 and M^* are known at the throat.

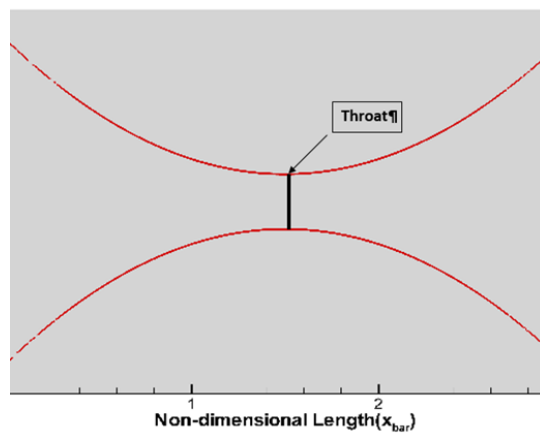


Figure 17. The throat (point of minimum cross-sectional area) of the nozzle where exact values are known

The values of T^*/T_0 , ρ^*/ρ_0 and M^* at the throat are 0.833, 0.528 and 1.0 respectively. Figures 18-20 show that the numerical solution gave the same results.

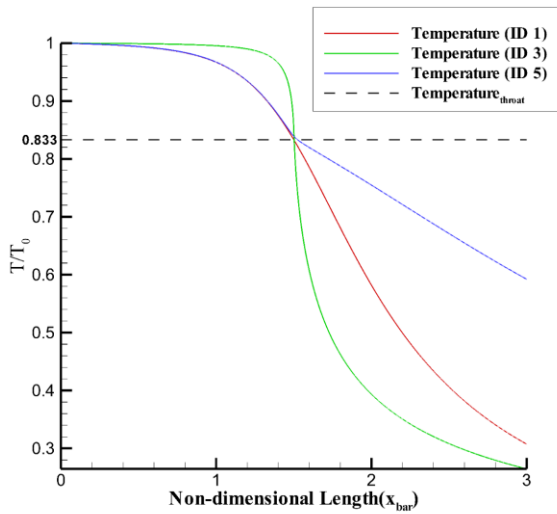


Figure 18. T^*/T_0 at the throat ($x_{bar} = 1.5$)

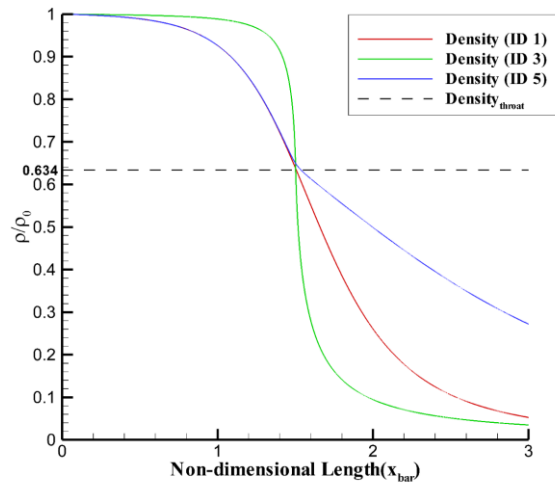


Figure 19. ρ^*/ρ_0 at the throat ($x_{bar} = 1.5$)

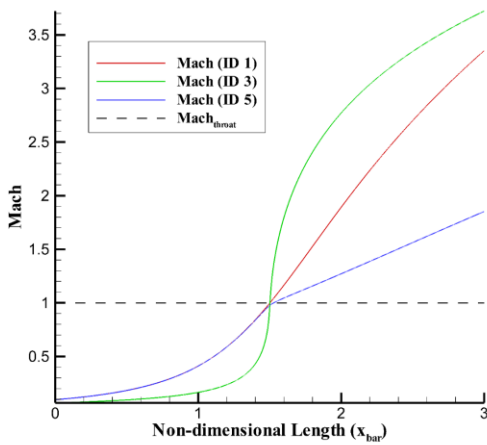


Figure 20. Mach number at the throat ($x_{bar} = 1.5$)

SECTION 4 DEMONSTRATING THE ACCURACY OF THE STANDARD SOLUTION

After verification and validation of the numerical solution, the numerical exact solution is given a grid sensitivity analysis to ensure that the solution does not change with change in grid size. For this project, the maximum grid at which the solution does not change with change in grid size was 5001 points. Figures 21-22 show that grid independence has been achieved.

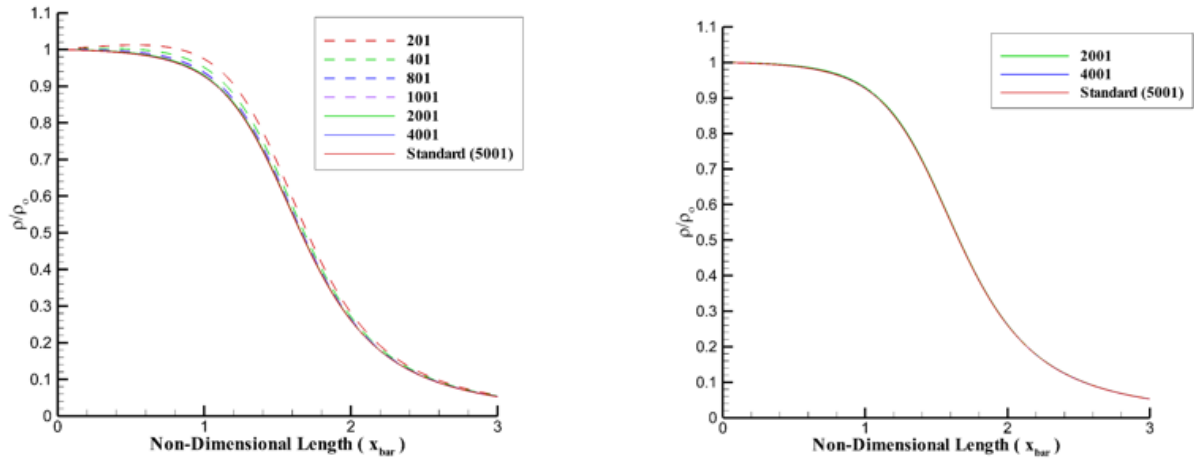


Figure 21. Grid independence analysis for Problem ID 1

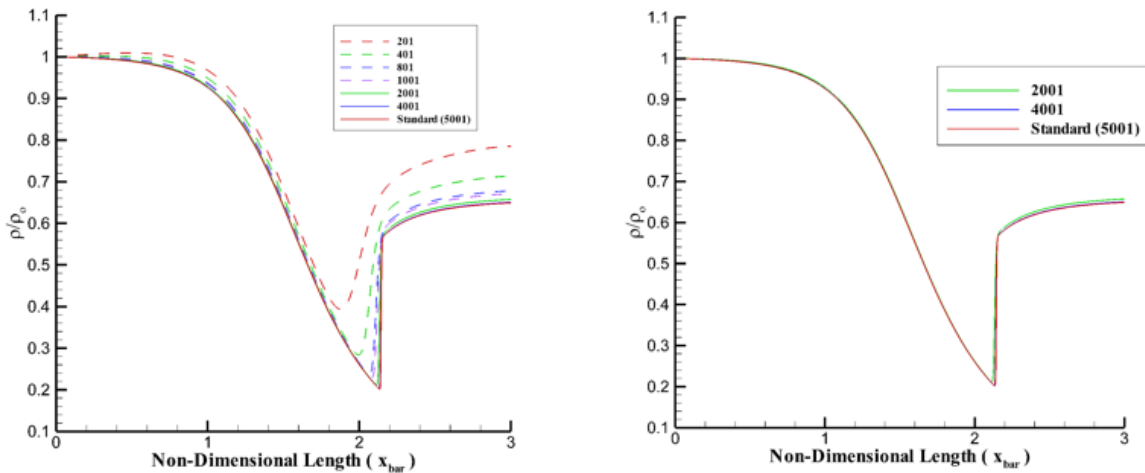


Figure 22. Grid independence analysis for Problem ID 2

Therefore we can conclude that the standard solution should have a grid size of 5001. For each geometry, the standard solution is expected to lie on each other for the isentropic and shock problem from the inlet until the shock wave is encountered. Behind the shock wave, the shock solution is expected to deviate from the isentropic solution since the shock solution is not reversible. Figures 23-27 demonstrate that the standard solution is qualitatively accurate.

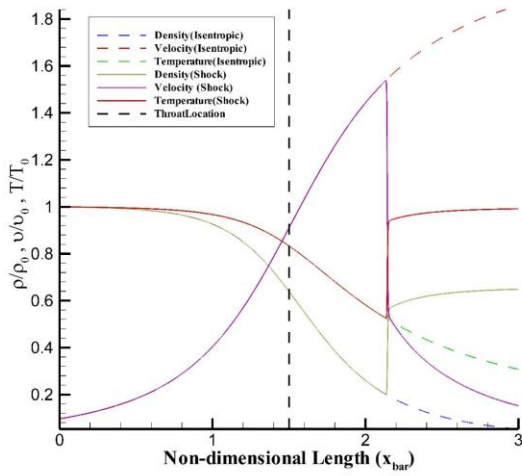


Figure 23: Standard solution for ID 1 and ID 2

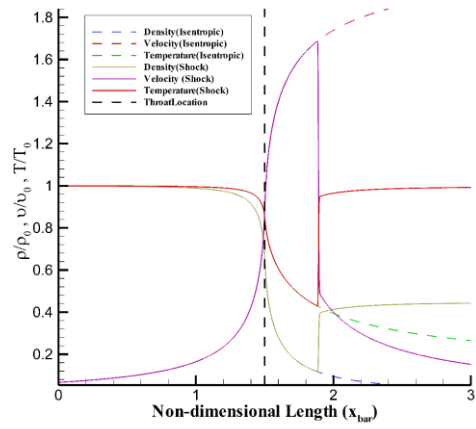


Figure 24: Standard solution for ID 3 and ID 4

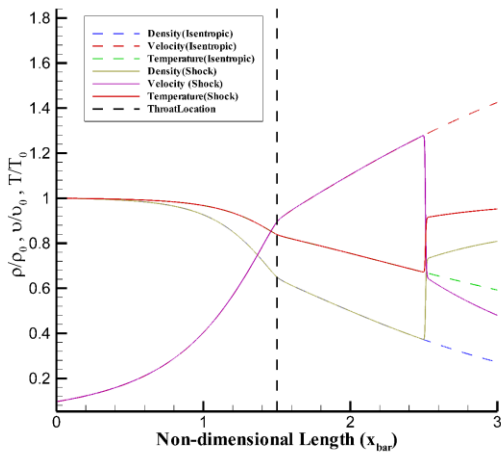


Figure 25: Standard solution for ID 5 and ID 6

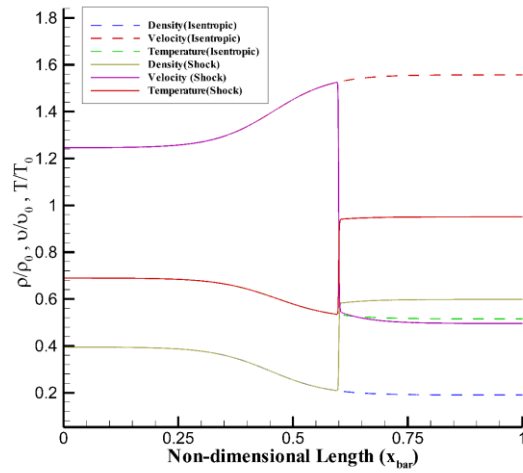


Figure 26: Standard solution for ID 7 and ID 8

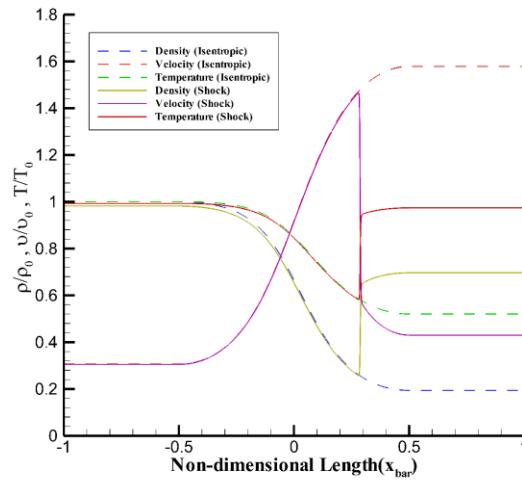


Figure 27: Standard solution for ID 9 and ID 10

Finally, a quantitative error analysis is performed. This is done by comparing the exact known values at the throat of the nozzle for the isentropic and shock solutions. And subsequently comparing the total temperature, total pressure and mass flow rate throughout the entire nozzle. The total pressure is not used for the shock problems since it is not conserved across the shock wave. Table 1 shows that the maximum percent error obtain for the isentropic problems is 6.7852%. Table 2 shows that the maximum percent error obtain for the shock problems is 6.6817%.

Table 1. Table of Error for Isentropic Problems

Common Assumptions : Numerical Standard Solution (Maximum Grid points : 5001) Tolerance (10 ⁻¹³)						
	Point data (Throat Location)			Distributed Data		
	$\varepsilon(T_o/T^*)\%$	$\varepsilon(P_o/P^*)\%$	$\varepsilon(M)\%$	$\sqrt{\frac{\sum_i^N(1.0 - T_o)^2}{\sum_i^N(1.0)^2}}$	$\sqrt{\frac{\sum_i^N(1.0 - P_o)^2}{\sum_i^N(1.0)^2}}$	$\sqrt{\frac{\sum_i^N(m_{exact} - m_i)^2}{\sum_i^N(m_{exact})^2}}$
1	1.1548e-02	8.2780e-01	3.2835e-01	1.3137E-003	4.5326E-003	4.7422E-003
3	2.0910	6.7852	4.6841	1.5456E-003	2.377E-002	3.1330E-002
5	6.9240e-01	3.1886	2.4376	1.1432E-003	4.8848E-003	3.9372E-003
9	2.0551	6.6931	0.4363	1.9058E-002	6.4387E-002	5.6816E-002
Max Error	2.0910	6.7852	4.6841	1.9058E-002	6.4387E-002	5.6816E-002

Table 2. Table of Error for Shock Problems

Problem ID	Point data			Distributed Data(L2 Norm)	
	$\varepsilon(T_o/T^*)\%$	$\varepsilon(P_o/P^*)\%$	$\varepsilon(M)\%$	$\sqrt{\frac{\sum_i^N (1.0 - T_0)^2}{\sum_i^N (1.0)^2}}$	$\sqrt{\frac{\sum_i^N (m_{exact} - m_i)^2}{\sum_i^N (m_{exact})^2}}$
2	9.5686e-04	8.1800e-01	3.0791e-01	2.9257E-003	1.0303E-002
4	2.0571	6.6744	4.6	3.5008E-003	3.4672E-002
6	6.7717e-01	3.0498	2.2890	1.1835E-003	4.5238E-003
8	-	-	-	2.0130E-003	6.5547E-003
10	2.0490	6.6817	0.4241	1.8957E-002	5.7761E-002
Max Error	2.0571	6.6817	4.6	1.8957E-002	5.7761E-002

CONCLUSIONS

The results show that the maximum error was 6.78% and occurred at the throat of the nozzle with an acute throat gradient. The sharp gradient introduced errors since the transition from subsonic flow speed to supersonic speed across the throat of a nozzle occurs over a smooth gradient. Thus the maximum error occurring at that location is expected. A maximum error of 6.78% can be considered minimal thus validating the use of the standard numerical solution as ‘quasi-exact’. The standard solution can therefore be used in place of an analytical solution for the purpose of error analysis.

REFERENCES

1. Ferguson, F. and G. Elamin, *A numerical solution of the NS equations based on the mean value theorem with applications to aerothermodynamics*. Advanced Computational Methods in Heat Transfer IX, 2006: p. 97.
2. Elamin, G.A., *The Integral-differential Scheme (IDS): A New CFD Solver for the System of the Navier-Stokes Equations with Applications*. 2008.
3. Anderson, J. D., & Wendt, J. (1995). *Computational fluid dynamics* (Vol. 206). New York: McGraw-Hill.
4. Hoffmann, K. A., & Chiang, S. T. (2000). *Computational Fluid Dynamics Volume II. Engineering Education System, Wichita, Kan, USA*.